Acta Crystallographica Section A
Foundations of Crystallography
ISSN 0108-7673

Received 12 September 2006
Accepted 13 December 2006

A direct phasing method based on the origin-free modulus sum function and the FFT algorithm. XII

Jordi Rius,* Anna Crespi and Xavier Torrelles

Institut de Ciència de Materials de Barcelona (CSIC), Campus de la UAB, 08193-Bellaterra, Catalunya, Spain. Correspondence e-mail: jordi.rius@icmab.es

An alternative way of refining phases with the origin-free modulus sum function S is shown that, instead of applying the tangent formula in sequential mode [Rius (1993). *Acta Cryst.* A**49**, 406–409], applies it in parallel mode with the help of the fast Fourier transform (FFT) algorithm. The test calculations performed on intensity data of small crystal structures at atomic resolution prove the convergence and hence the viability of the procedure. This new procedure called S-FFT is valid for all space groups and especially competitive for low-symmetry ones. It works well when the charge-density peaks in the crystal structure have the same sign, *i.e.* either positive or negative.

1. Introduction

Recently, it was shown that the maximum-likelihood estimate of the phases of the structure factors corresponds to the maximum of the likelihood function L (Rius, 2006), which after some approximations can be simplified to

$$L(\Phi) \simeq c \prod_{\mathbf{H}} \exp\{(|G_{\mathbf{H}}| - \langle|G|\rangle)|G_{\mathbf{H}}(\Phi)|/\sigma^2_{\mathbf{H}}\}. \quad (1)$$

$|G_{\mathbf{H}}|$ and $|G_{\mathbf{H}}(\Phi)|$ are, respectively, the observed and calculated structure-factor amplitudes of the squared electron-density distribution (ρ^2) with associated phases $\psi_{\mathbf{H}}$ and c is a scaling constant. The symbol **H** stands for both the strongest and weakest reflections, while Φ denotes the collectivity of phases $\varphi_{\mathbf{h}}$ associated with the amplitudes $|E_{\mathbf{h}}|$ of the largest **h** reflections corresponding to the electron-density distribution (ρ). In practice, the $|G_{\mathbf{H}}|$ are not directly measurable quantities. However, if it is assumed for simplicity that ρ corresponds to a crystal structure with N equal atoms in the unit cell following $P1$ space-group symmetry, they can be derived from the observed $|E|$ values through the simple relationship $|G_{\mathbf{H}}| = (1/N^{1/2})|E_{\mathbf{H}}|$. Hence, expression (1) becomes

$$L(\Phi) \simeq c \prod_{\mathbf{H}} \exp\{(1/N^{1/2})(|E_{\mathbf{H}}| - \langle|E|\rangle)|G_{\mathbf{H}}(\Phi)|/\sigma^2_{\mathbf{H}}\}. \quad (2)$$

If the $\sigma^2_{\mathbf{H}}$ are assumed to be equal for all **H**, the scaling constant $K = N^{-1/2}\sigma^{-2}$ can be introduced and, by adding the exponents, the origin-free modulus sum function results:

$$S = K \sum_{\mathbf{H}} [|E_{\mathbf{H}}| - \langle|E|\rangle]|G_{\mathbf{H}}(\Phi)|. \quad (3)$$

Since the maximum of S corresponds to the maximum of L, the refined Φ maximizing S will give the maximum-likelihood estimate of the phases. To find the Φ maximizing S, the phase $\psi_{\mathbf{H}} = f(\Phi)$ of the complex conjugate of $G_{-\mathbf{H}}(\Phi)$ is introduced. Then (3) can be expressed as

$$S = K \sum_{\mathbf{H}} [|E_{\mathbf{H}}| - \langle|E|\rangle] \exp(i\psi_{\mathbf{H}}) G_{-\mathbf{H}}(\Phi). \quad (4)$$

From Fourier theory, $G_{-\mathbf{H}}$ can be expressed in terms of the Fourier coefficients of ρ,

$$G_{-\mathbf{H}}(\Phi) = V^{-1} \sum_{\mathbf{h}} |E_{-\mathbf{h}}||E_{-\mathbf{H}+\mathbf{h}}| \exp i(\varphi_{-\mathbf{h}} + \varphi_{-\mathbf{H}+\mathbf{h}}), \quad (5)$$

so that in view of (5), (4) becomes

$$S = (K/V) \sum_{\mathbf{H}} (|E_{\mathbf{H}|} - \langle|E|\rangle) \exp(i\psi_{\mathbf{H}}) \times \sum_{\mathbf{h}} |E_{-\mathbf{h}}||E_{\mathbf{h}-\mathbf{H}}| \exp i(\varphi_{-\mathbf{h}} + \varphi_{\mathbf{h}-\mathbf{H}}). \quad (6)$$

Finally, rearranging the summations in (6), it follows that

$$S = \sum_{\mathbf{h}} |E_{-\mathbf{h}}| \exp(i\varphi_{-\mathbf{h}}) \left[(K/V) \sum_{\mathbf{H}} (|E_{\mathbf{H}}| - \langle|E|\rangle) \exp(i\psi_{\mathbf{H}}) E_{\mathbf{h}-\mathbf{H}} \right]. \quad (7)$$

One way of maximizing S is by means of improved tangent formulae (TF). In practice, there are two possible modes of performing a TF phase refinement.

(i) *The sequential mode.* The initial set Φ of random phase values is introduced in the TF. In this way, a first estimate of the phase $\varphi_{\mathbf{h}}$ is obtained. This new value replaces the old value in Φ. With the updated Φ, the φ value of the next reflection is computed. This process is repeated until all **h** reflections in the file have been treated. If there are still changes, the refinement starts again with the first **h** reflection until no modifications are observed. This sequential mode is very effective and can be easily applied in reciprocal space (Debaerdemaeker *et al.*, 1985; Rius, 1993). From (7), it follows that, when the value of $\varphi_{\mathbf{h}}$ is equal to the phase value of the summation $\sum_{\mathbf{H}}(|E_{\mathbf{H}}| - \langle|E|\rangle) \exp(i\psi_{\mathbf{H}})\, E_{\mathbf{h}-\mathbf{H}}$ (with **H** including both large and weak reflections), then S is maximal. Notice that for large crystal structures the total number of terms in the summation becomes prohibitive. Introducing a higher cut-off limit for the E values in expression (5), *e.g.* 1.6 instead of 1.35, reduces this

Table 1
Relevant crystal data of the compounds selected for checking the viability of the S-FFT phase refinement procedure; the resolution limit is given by the d spacing in Å and B is the overall temperature parameter in Å^2.

Code	Unit-cell content	Space group	d	B
PGE2[a]	$C_{20}H_{32}O_5$	$P1$	1.00	5.6
MBH2[b]	$C_{45}H_{72}O_9$	$P1$	0.85	4.7
TVAL[c]	$C_{108}H_{180}N_{12}O_{36}$	$P1$	0.82	5.4
NEWQB[d]	$C_{96}H_{80}N_8O_{20}$	$P\bar{1}$ as $P1$	1.04	2.2
GOLDMAN2[e]	$C_{224}H_{128}$	Cc	0.76	3.3
BHAT[f]	$C_{20}H_{16}F_8N_{20}O_{36}$	Pc	0.86	4.0
HOV1[g]	$Pr_{56}Ni_{32}Si_{36}$	$C2/m$ as Cm	0.78	0.6
MUNICH1[h]	$C_{160}H_{128}$	$C2$	0.89	3.8
BIH[i]	$C_{56}H_{152}B_{36}O_{12}N_4S_8$	$P2_1/c$ as Pc	0.84	3.6
CORTISON[j]	$C_{84}H_{112}O_{20}$	$P2_12_12_1$	0.89	3.3
BNA[k]	$C_{40}B_{36}H_{100}Na_4O_{12}S_8$	$Pnma$ as $P2_12_12_1$	0.84	3.9
WINTER2[l]	$C_{110}H_{178}Cl_{12}N_{22}O_{32}$	$P2_1$	0.84	6.6
TOTC[m]	$C_{198}H_{216}O_{36}$	$P6_1$	1.00	4.7
TUR10[n]	$C_{180}H_{288}O_{24}$	$P6_322$	1.00	4.2
BED[o]	$C_{208}H_{208}N_{32}O_{32}$	$I4$	0.90	4.1
ALFA1[p]	$C_{328}H_{500}N_{65}O_{110}$	$P1$	0.90	4.2

References: (*a*) DeTitta *et al.* (1980); (*b*) Poyser *et al.* (1986); (*c*) Smith *et al.* (1975); (*d*) Grigg *et al.* (1978); (*e*) Irngartinger *et al.* (1981); (*f*) Bhat & Ammon (1990); (*g*) Hovestreydt *et al.* (1983); (*h*) Szeimies-Seebach *et al.* (1978); (*i*) Teixidor *et al.* (1991); (*j*) Declercq *et al.* (1972); (*k*) Teixidor *et al.* (1990); (*l*) Butters *et al.* (1981); (*m*) Williams & Lawton (1975); (*n*) Braekman *et al.* (1981); (*o*) Sheldrick *et al.* (1978); (*p*) Privé *et al.* (1999).

number at the cost of lowering the accuracy of the calculated $G(\Phi)$'s.

(ii) *The parallel mode.* Like in mode (i), the initial set Φ of random phases is introduced in the TF and the first estimate of $\varphi_{\mathbf{h}}$ obtained. The new value of $\varphi_{\mathbf{h}}$ is then stored without updating Φ, so that the phase value of the next **h** reflection is still determined with the initial set Φ of phase values. Only when all **h** reflections have been treated will Φ be updated. This process is repeated until no more significant changes in the phase values are observed. Since all phase values are computed from the same Φ, this calculation can be done applying the FFT algorithm. In the next section, such a procedure is described.

To avoid confusion, the procedure maximizing S with the tangent formula in sequential mode will be called S-TF, while the one based on the parallel mode will be denoted by S-FFT.

2. The S-FFT phase refinement method

First let the expression

$$D_{\mathbf{H}}(\Phi) = (|E_{\mathbf{H}}| - \langle|E|\rangle)\exp(i\psi_{\mathbf{H}}) \tag{8}$$

in (7) represent the Fourier coefficients of the modified electron-density function $\rho'_{\rm sq}$. Then (7) can be written in the more compact form

$$S = K\sum_{\mathbf{h}} E_{-\mathbf{h}}\left[V^{-1}\sum_{\mathbf{H}} D_{\mathbf{H}}(\Phi)E_{\mathbf{h}-\mathbf{H}}\right] \tag{9}$$

$$= K\sum_{\mathbf{h}} |E_{-\mathbf{h}}|\exp(i\varphi_{-\mathbf{h}})Q_{\mathbf{h}}(\Phi). \tag{10}$$

The magnitudes $Q_{\mathbf{H}}(\Phi)$ represent the Fourier coefficients of the product function

$$\rho_m(\Phi) = \rho'_{\rm sq}(\Phi)\rho(\Phi), \tag{11}$$

that is

$$Q_{\mathbf{H}}(\Phi) = \int_v \rho_m(\Phi)\exp(i2\pi\mathbf{Hr})\,{\rm d}V. \tag{12}$$

It is obvious from the analysis of (10) that, for a fixed set of $Q_{\mathbf{h}}(\Phi)$ magnitudes, the new estimates of φ maximizing S can be obtained from the tangent formula

$$\varphi_{\mathbf{h}({\rm new})} = \text{phase of } \{Q_{\mathbf{h}}(\Phi_{\rm old})\}. \tag{13}$$

In practice, all $Q_{\mathbf{H}}(\Phi_{\rm old})$ and, consequently, all new phase estimates φ, are calculated simultaneously applying the FFT algorithm to (12). Moreover, since the S-FFT procedure does not involve the condition $\psi_{\mathbf{h}} = \varphi_{\mathbf{h}}$, the refinement can produce either ρ or $-\rho$ as solutions when starting from random phases. The details of the iterative S-FFT phase refinement procedure are described in Fig. 1. However, since this procedure supplies all new $\varphi_{\mathbf{h}}$ values at the same time, no warranty exists that, when substituting all these new $\varphi_{\mathbf{h}}$ estimates to give $\Phi_{\rm new}$, $S(\Phi_{\rm new})$ will be a maximum. Consequently, it is necessary to check the convergence of this iterative procedure experimentally. To follow the convergence during the phase refinement, the correlation coefficient

$${\rm CC} = \left[\sum_{\mathbf{H}} |E_{\mathbf{H}}||Q_{\mathbf{H}}(\Phi)|\right]^2 \Big/ \left\{\left[\sum_{\mathbf{H}} |E_{\mathbf{H}}|^2\right]\left[\sum_{\mathbf{H}} |Q_{\mathbf{H}}(\Phi)|^2\right]\right\} \tag{14}$$

is used as figure of merit. The refinement stops when no more significant changes in CC are observed or, alternatively, a given preset number of cycles is reached. At the end, to discriminate between the positive and negative crystal structure solutions, the fraction of negative pixels in ρ_m is calculated. If the fraction lies in the 0.28–0.30 range, the positive solution has been reached; on the contrary, if the fraction falls between 0.70 and 0.72, the negative solution has been refined and, consequently, π rad must be added to the refined phase values to get the positive solution.

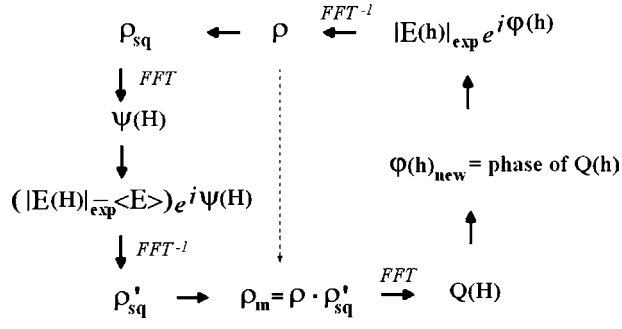

Figure 1
Iterative S-FFT phase refinement procedure. The initial phases (upper right corner) are combined with the experimental amplitudes to compute the electron density ρ. Most existing FFT-based structure-solution methods manipulate ρ in real space (broken arrow) to yield a modified one, ρ_m. In the S-FFT procedure, this modification is done automatically with the help of two additional Fourier transforms (at the left). The Fourier transform of ρ_m yields the new structure-factor estimates.

Table 2
Compound TVAL: number of successful trials out of a total of 25 for different $\langle|E|\rangle$ and $|E|_{\rm lim}$.

The respective CC values for the correct and wrong solutions were 0.87 and 0.83 (for $|E|_{\rm lim} = 1.35$) and 0.88 and 0.85 (for $|E|_{\rm lim} = 1.25$). The results in this table show the tolerance of the S-FFT refinement to different $\langle|E|\rangle$ values.

	Average $\|E\|$ value				
$\|E\|_{\rm lim}$	0.85	0.90	1.00	1.10	1.20
1.35	23	24	23	17	14
1.25	23	23	25	21	14

3. Test calculations

The test calculations were performed on the intensity data of the crystal structures summarized in Table 1.

A first series of test calculations was carried out to check the influence of the $\langle|E|\rangle$ value on the effectiveness of the S-FFT phase refinement. It is known that the $\langle|E|\rangle$ values normally employed when refining with the S-TF lie between 0.85 and 1.05, which are the values that result for an approximately equal number of large and weak reflections. In general, the S-TF refinement is rather insensitive to the particular value of $\langle|E|\rangle$ used provided that it falls within this interval. To confirm that the S-FFT refinement behaves in a similar way, some calculations with different $\langle|E|\rangle$ values and two cut-off values $|E|_{\rm lim}$ were carried out. The results given in Table 2 confirm the expected similarity.

The aim of the second series of test calculations is to prove the convergence and hence the viability of the S-FFT phase refinement. To this purpose, the *XLENS* program (Rius, 1993) was modified to incorporate the S-FFT phase-refinement procedure described in Fig. 1. At the beginning of each cycle, the new ρ values are computed using the largest structure factors only. Table 3 lists the test results. To make comparison between calculations from different crystal structures easier, the $\langle|E|\rangle$ values were arbitrarily fixed to one. This was achieved by selecting only those large reflections with $|E|$ values greater than $|E|_{\rm lim} = 1.35$ and adjusting the number of weak $|E|$ values to give $\langle|E|\rangle \simeq 1$. Inspection of Table 3 shows that both convergence and number of successful trials is excellent for small crystal structures refined in $P1$ and for compounds allowing the origin of the unit cell to float on a plane. Table 3 also includes additional test calculations for space groups having the unit-cell origin fixed or restricted to one dimension. In general, the number of successful trials is here much lower. This is not surprising since a similar behaviour was already found some years ago when studying the practical application of the S-TF (Rius *et al.*, 1995). Table 3 also indicates that the number of successful trials obtained with the S-FFT and the S-TF is similar for all test structures. A point of practical importance is that, for a given structure, the correct solutions of the S-FFT procedure converged to the same CC value, *i.e.* to the largest value that falls between 0.85 and 0.93 depending on the data resolution. Although the purpose of the present contribution is not an exhaustive check on the applicability of the S-FFT to large crystal structures, a preliminary test on the polypeptide ALFA1 has been performed using the same refinement parameters as for the smaller crystal structures. It can be seen in Table 3 that one solution is produced every 120 trials. The average CPU time for one trial, in a rather old computer (Pentium 3, 800 MHz, Ram 256 Mb, 32 bits Fortran compiler), is 16 min for ALFA1 ($\leq$179 cycles), 1.2 min for TVAL ($\leq$87 cycles) and 20 s for MBH2 ($\leq$64 cycles). For the S-TF approach, the corresponding CPU times are 2.5 s for TVAL and 1 s for MBH2.

Table 3
Results of the S-FFT phase refinement procedure for different compounds.

The respective data resolution limits are the d values given in Table 1. In all cases, the number of weak $|E|$'s was chosen to give $\langle|E|\rangle = 1$. The range of cycles per trial given is based on the end criterion ($|\Delta{\rm CC}| < 0.0003$ for the last two cycles). The last column indicates the number of solutions with positive electron density. It can be seen that both S-FFT and S-TF procedures yield similar success ratios, although the S-TF is much more efficient in computing time.

Code	No. of refined phases	No. of weak |E|'s	No. of solutions with S-FFT/ S-TF	No. of trials and (cycles)	No. of solutions with positive ρ
PGE2	161	175	21 / 25	25 (11–37)	11
MBH2	580	557	24 / 24	25 (15–70)	12
TVAL	1043	1253	23 / 25	25 (19–54)	17
NEWQB	663	638	24 / 25	25 (21–60)	15
GOLDMAN2	607	583	25 / 25	25 (16–45)	9
BHAT	285	269	11 / 16	25 (24–49)	3
HOV1	518	496	22 / 25	25 (14–67)	14
MUNICH1	352	333	2 / 2	50 (18–55)	0
BIH	661	636	25 / 25	25 (10–20)	16
CORTISON	247	231	6 / 14	50 (17–47)	1
BNA	303	286	5 / 7	25 (9–12)	2
WINTER2	1045	1013	6 / 1	25 (30–53)	1
TOTC	301	284	20 / 25	25 (17–51)	8
TUR10	160	150	6 / 8	50 (20 fixed)	3
BED	285	268	8 / 8	25 (18–50)	5
ALFA1	3772	3771	3 / †	360 (88–179)	0

† The S-TF refinement with the same control parameters could not be done due to the large number of triplets generated.

4. Conclusions

A new direct phasing method based on the maximization of the origin-free modulus sum function with the TF in parallel mode computed using the FFT algorithm has been derived. This method requires (i) the charge density to be either positive or negative in order to allow the derivation of the moduli $|G_{\mathbf{H}}|$ from the experimental $|E_{\mathbf{H}}|$ and (ii) the resolution of the intensity data to be high enough to produce accurate calculated amplitudes $|G_{-\mathbf{H}}(\Phi)| = \exp(i\psi_{\mathbf{H}})G_{-\mathbf{H}}(\Phi)$. Since no explicit use of the condition $\psi_{\mathbf{h}} = \varphi_{\mathbf{h}}$ is made, the procedure can supply either the positive or the negative correct solution. This could be useful for example in single-crystal neutron diffraction studies for unit cells with the protons being the dominant scatterers.

From the analysis of the test calculations, it can be concluded that: (i) the degree of convergence of TF refinements in parallel and sequential mode is similar at least for

small crystal structures; (ii) for small crystal structures, TF refinement in sequential mode is faster, although this is not very important in practice due to the high success ratios (especially for low-symmetry space groups); (iii) for medium-scale crystal structures, the S-FFT refinement imposes no limitation on the cut-off limit of the large E values. This difference with respect to the S-TF is very important, since the principal limitation of the latter, that is the inaccuracy of $G(\Phi)$, disappears. The application of the S-FFT refinement to large structures will be the subject of a separate investigation.

In the literature, there are other *ab initio* crystal-structure-solution algorithms alternating between real and reciprocal space, making use of the Fourier transform and doing part of the job by imposing constraints on the electron density (Miller *et al.*, 1993; Brenner *et al.*, 1997; Sheldrick, 1998; Oszlányi & Sütő, 2004, 2005). One of the peculiarities of the method described here is that the modification of the electron density is not performed in real space but involves an additional reciprocal-space part. This causes the computation to be somewhat lengthier, but as a counterpart the method converges quickly without the previous estimation of empirical parameters. This should offer new possibilities in fields like powder and surface X-ray diffraction where the electron density can be easily modified in real space, thus enabling additional control of the phase-refinement process (Baerlocher *et al.*, 2006). In this way, methods like the one based on the S-TF and described in Rius *et al.* (2000) for the treatment of accidental peak overlap in powder diffraction could be reformulated and worked out more easily.

This work was supported by the Spanish 'Ministerio de Eduación y Ciencia' Project No. MAT2005-01736 and by the 'Generalitat de Catalunya' (SGR2005-00452). Thanks are due to the referees for valuable suggestions.

References

Baerlocher, Ch., McCusker, L. B. & Palatinus, L. (2006). *EPDIC-10 Abstracts Book*, p. 18.
Bhat, T. N. & Ammon, H. L. (1990). *Acta Cryst.* C**46**, 112–116.
Braekman, J. C., Daloze, D., Dupont, A., Tursch, J. P., Declercq, J. P., Germain, G. & Van Meersche, M. (1981). *Tetrahedron*, **37**, 179–186.
Brenner, S., McCusker, L. B. & Baerlocher, Ch. (1997). *J. Appl. Cryst.* **30**, 1167–1172.
Butters, T., Hütter, P., Jung, G., Pauls, N., Schmitt, H., Sheldrick, G. M. & Winter, W. (1981). *Angew. Chem.* **93**, 904–905.
Debaerdemaeker, T., Tate, C. & Woolfson, M. M. (1985). *Acta Cryst.* A**41**, 286–290.
Declercq, J. P., Germain, G. & Van Meersche, M. (1972). *Cryst. Struct. Commun.* **1**, 13–15.
DeTitta, G. T., Langs, D. A., Edmonds, J. W. & Duax, W. L. (1980). *Acta Cryst.* B**36**, 638–645.
Grigg, R., Kemp, J., Sheldrick, G. M. & Trotter, J. (1978). *J. Chem. Soc. Chem. Commun.* pp. 109–111.
Hovestreydt, E., Klepp, K. & Parthé, E. (1983). *Acta Cryst.* C**39**, 422–425.
Irngartinger, H., Reibel, W. R. K. & Sheldrick, G. M. (1981). *Acta Cryst.* B**37**, 1768–1771.
Miller, R., DeTitta, G. T., Jones, R., Langs, D. A., Weeks, C. M. & Hauptman, H. A. (1993). *Science*, **259**, 1430–1433.
Oszlányi, G. & Sütő, A. (2004). *Acta Cryst.* A**60**, 134–141.
Oszlányi, G. & Sütő, A. (2005). *Acta Cryst.* A**61**, 147–152.
Poyser, J. P., Edwards, P. L., Anderson, J. R., Hursthouse, M. B., Walker, N. P. C., Sheldrick, G. M. & Whalley, A. J. S. (1986). *J. Antibiot.* **39**, 167–169.
Privé, G. G., Anderson, D. H., Wesson, L., Cascio, D. & Eisenberg, D. (1999). *Protein Sci.* **8**, 1–9.
Rius, J. (1993). *Acta Cryst.* A**49**, 406–409.
Rius, J. (2006). *Acta Cryst.* A**62**, 331–335.
Rius, J., Sañé, J., Miravitlles, C., Amigó, J. M. & Reventós, M. M. (1995). *Acta Cryst.* A**51**, 268–270.
Rius, J., Torrelles, X., Miravitlles, C., Ochando, L. E., Reventós, M. M. & Amigó, J. M. (2000). *J. Appl. Cryst.* **33**, 1208–1211.
Sheldrick, G. M. (1998) *Direct Methods for Solving Macromolecular Structures*, edited by S. Fortier, pp. 401–411. Dordrecht: Kluwer Academic Publishers.
Sheldrick, G. M., Davison, B. E. & Trotter, J. (1978). *Acta Cryst.* B**34**, 1387–1389.
Smith, G. D., Duax, W. L., Langs, D. A., DeTitta, G. T., Edmonds, J. W., Rohrer, D. C. & Weeks, C. M. (1975). *J. Am. Chem. Soc.* **97**, 7242–7247.
Szeimies-Seebach, U., Harnisch, J., Szeimies, G., Van Meersche, M., Germain, G. & Declercq, J. P. (1978). *Angew. Chem. Int. Ed. Engl.* **17**, 848–850.
Teixidor, F., Rius, J., Romerosa, A., Miravitlles, C., Escriche, L. L., Sanchez, E., Viñas, C. & Casabó, J. (1991). *Inorg. Chim. Acta*, **176**, 61–65.
Teixidor, F., Viñas, C., Rius, J., Miravitlles, C. & Casabó, J. (1990). *Inorg. Chem.* **29**, 149–152.
Williams, D. J. & Lawton, D. (1975). *Tetrahedron Lett.* pp. 111–114.